International Journal of Modern Physics A
Vol. 29, No. 7 (2014) 1460003 (34 pages)

DOI: 10.1142/S0217751X14600033

Why has global warming paused?*

William Happer
Department of Physics, Princeton University, Princeton, NJ 08544, USA
happer@princeton.edu

Received 29 November 2013
Revised 10 February 2014
Accepted 13 February 2014
Published 11 March 2014

1. Introduction

Freeman Dyson has been interested in climate for most of his life. He coauthored one of the earliest books on the interplay of CO_2 and climate in 1982:

> "The Long-term Impacts of Increasing Atmospheric Carbon Dioxide Levels", edited by Gordon J. MacDonald (Ballinger Publishing Company, 2008).

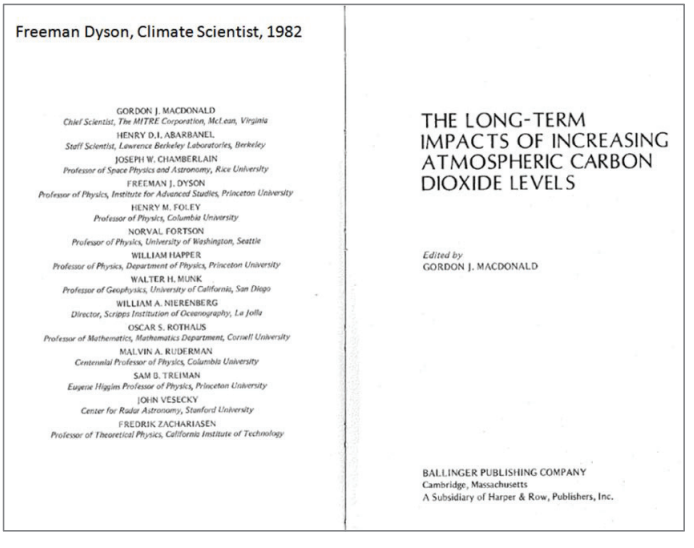

Slide 1.

*Based on a talk given at the conference *Dreams of Earth and Sky: A Celebration for Freeman Dyson*, Institute for Advanced Study, Princeton, 27 September 2013.

The version of the NASA picture "retouched" by Richard Petrucci for Al Gore's book "Our Choice."

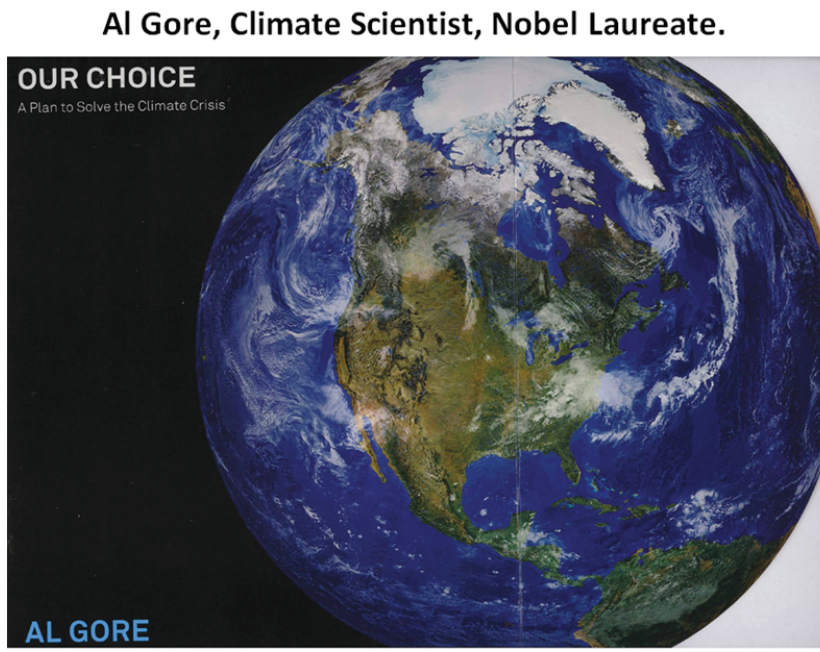

Slide 2. The version of the NASA picture "retouched" by Richard Petrucci for Al Gore's book "Our Choice."

1. Much of the cloud cover has been removed, especially in the Arctic and South America. This belittles the enormous influence of cloud albedo on the radiative forcing of the earth.
2. An ice free Arctic shore of Siberia has been added, and other changes have been made to make the Arctic ocean appear to have more ice-free water.
3. Daylight has been added to the eastern and northern edges of the photo, which were originally in twilight or dark. We now have a perfectly "limb-brightened" earth.

Slide 3. The original for the image on the Book's cover (Slide 2).
http://www.google.com/#q=pictures+of+earth+from+space+nasa

From the cloud patterns, it is clear that this is the original of the cover picture of Al Gore's book "Our Choice," Melcher Media, New York, 2009.

See the post:
http://wattsupwiththat.com/2009/11/19/not-finding-any-gore-airbrushes-in-hurricanes-for-his-new-book/

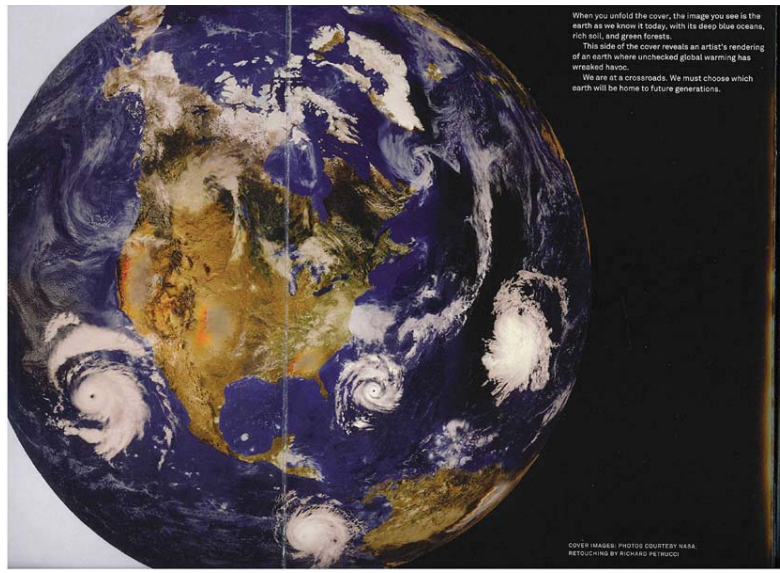

Slide 4. The image on the inner cover showing the lamentable effects of more CO_2.

Al Gore's vision of the future, the inner part of the front cover of "Our Choice," including:

1. A hurricane spiraling the wrong way off the US east coast. Politicians have repealed the pesky law of conservation of angular momentum.
2. There is a hurricane off the equatorial coast of South America, spiraling the right way for the northern hemisphere. Before Al and his "scientists" abolished the law of conservation of angular momentum, hurricanes did not form within about plus or minus 10 degrees of the equator. The Coriolis force, which is needed to make hurricanes rotate, is zero at the equator.
3. The ice cover of the Arctic ocean is all gone, and a good fraction of the central part of Greenland is flooded, presumably because Al and his "scientists" looked up the current topography of Greenland. Of course you have to repeal another law of physics, isostatic glacial adjustment, which would require much of the interior parts of Greenland that are now below sea level to rise above sea level when the enormous weight of the ice cover is removed.
4. Much of Florida is under water.

5. Much of the US landmass is desert, including the southeast, which has somehow been transformed in to a desert in spite of getting more drenching "superstorms" like Sandy.
6. Except for hurricanes, there is almost no cloud cover.

Al Gore and many other politicians who have hitched their wagons to global warming have called those like Freeman Dyson who raise any questions "flat-earthers." Here is a birthday greeting to Freeman from his fellow flat-earther Harrison Schmitt. Harrison also served as Senator from the State of New Mexico after retiring from NASA.

Birthday Greetings to Freeman from Astronaut Harrison Schmitt:

"Please wish Freeman a Happy 90th Birthday for me. We met many years ago when I visited Princeton, and I have been an admirer for many reasons, from astrophysics, to strategic defense, to issues with climate modelling."

Photo taken by Harrison "at About 4 am ET, ..., at the first opportunity we were set up to coast to the moon. As you can see it is not a truly full Earth. We were still too close for that. Also, our trajectory to a 23 North latitude on the moon required that we view the southern hemisphere of the Earth more that the northern."

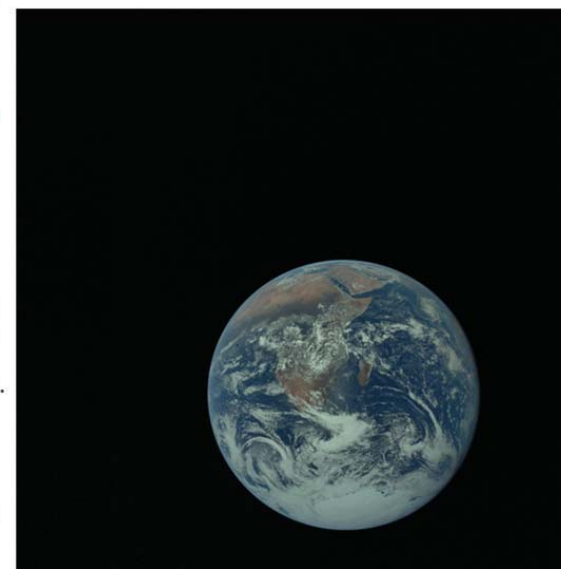

Slide 5.

How much global warming will come from additional CO_2? As this figure shows, CO_2 has been increasing steadily, and at least some of the increase is from the burning of fossil fuels, coal, oil, natural gas. This will cause some warming, but how much? As you can see from this figure, the mean temperature, shown in blue, has trends that are vaguely similar to that of CO_2, shown in red. But there is also a strong correlation with the phase of the Pacific Decadal Oscillation, shown on the bottom of the graph (Slide 6).

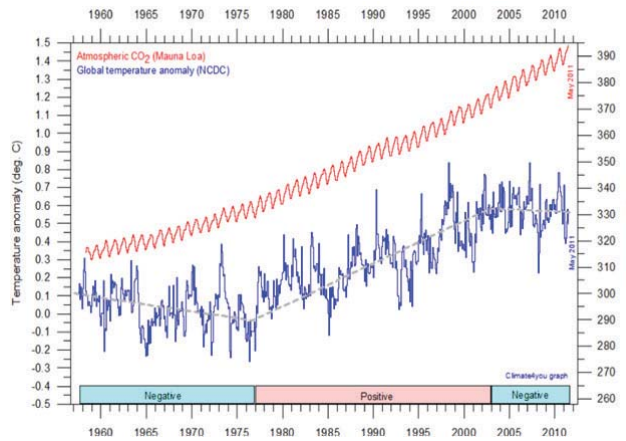

Slide 6.

Many independent instrumental records show that the relatively rapid temperature rise that began in the 1970's came to an end by the year 2000.

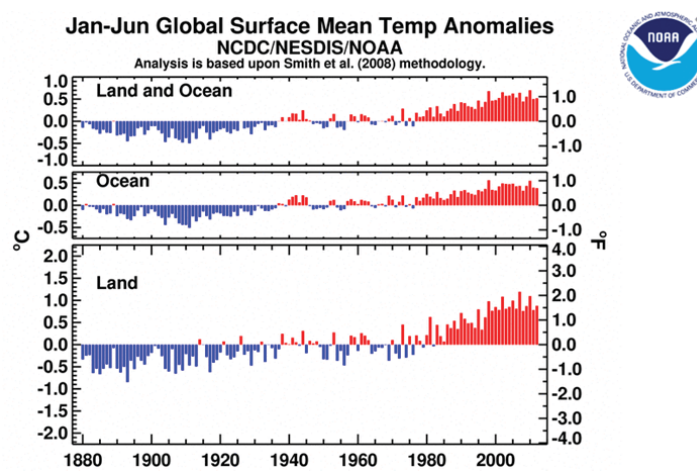

Slide 7.

Der Spiegel, Jan. 2013 **The press is beginning to notice the problem!**

Klimawandel: Forscher rätseln über Stillstand bei Erderwärmung

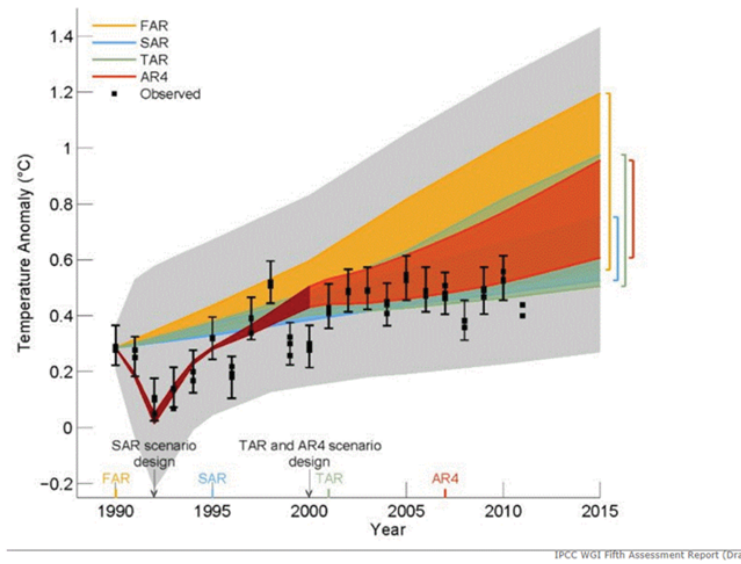

Slide 8.

Not only skeptics of global warming hysteria but even the popular press is beginning to notice that the predicted warming of IPCC models is much greater than what has been observed. This figure was published last year in the progressive German magazine, Der Spiegel, with the title: "Climate Change: Researchers are puzzled by the pause of global warming."

And it is not just the popular press that has noticed that earth is no longer warming, as you can see from the figures in a recent article from Nature, long a loyal promoter of alarming papers on global warming (Slide 9).

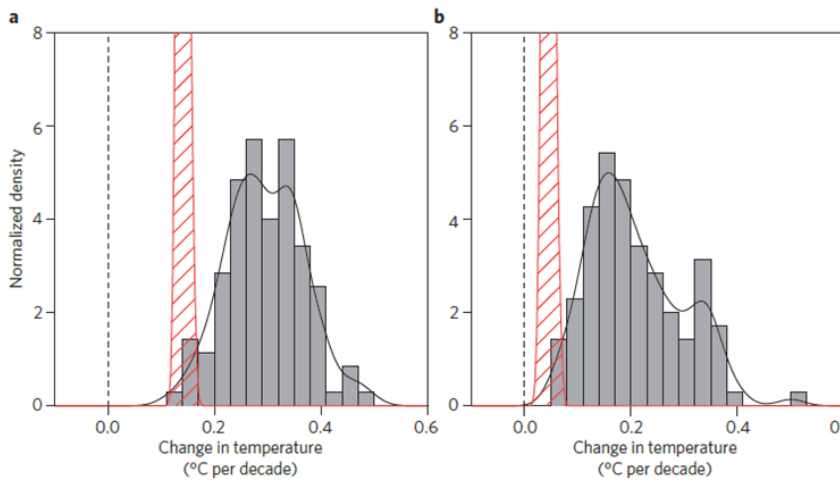

Figure 1 | Trends in global mean surface temperature. **a**, 1993–2012. **b**, 1998–2012. Histograms of observed trends (red hatching) are from 100 reconstructions of the HadCRUT4 dataset[1]. Histograms of model trends (grey bars) are based on 117 simulations of the models, and black curves are smoothed versions of the model trends. The ranges of observed trends reflect observational uncertainty, whereas the ranges of model trends reflect forcing uncertainty, as well as differences in individual model responses to external forcings and uncertainty arising from internal climate variability.

Nature Climate Change, Vol 3, p. 767, September 2013.

Slide 9.

Let us briefly review the basic physics of what determines the surface temperature of the earth. As shown in the sketch below (Slide 10), except for a very small amount of geothermal heat, the earth's surface is heated by sunlight with wavelengths of order half a micron, characteristic of the 5525 K blackbody temperature of the sun's surface, and by backradiation of infrared radiation from the atmosphere. The earth's surface is cooled mainly by convection, including cooling from the evaporation of water. Especially at night, the surface also cools by radiating directly to space in the thermal infrared window, with wavelengths of order 10 microns. The thermal radiation is characteristic of the approximately 300 K surface temperature of the earth. Most of the thermal radiation to space does not come from the surface but from higher altitudes, from greenhouse gases, predominantly H_2O and CO_2, and from clouds or other particulates.

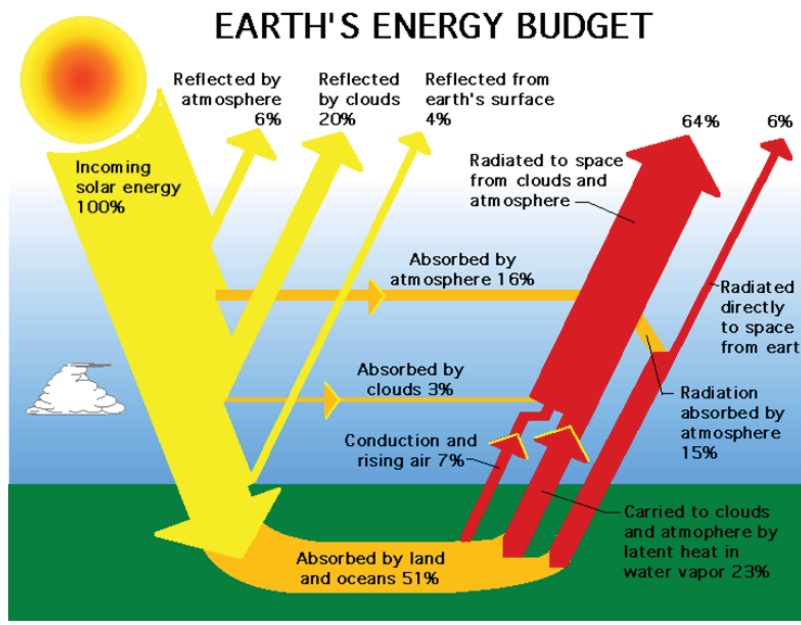

Slide 10. earth energy budget.

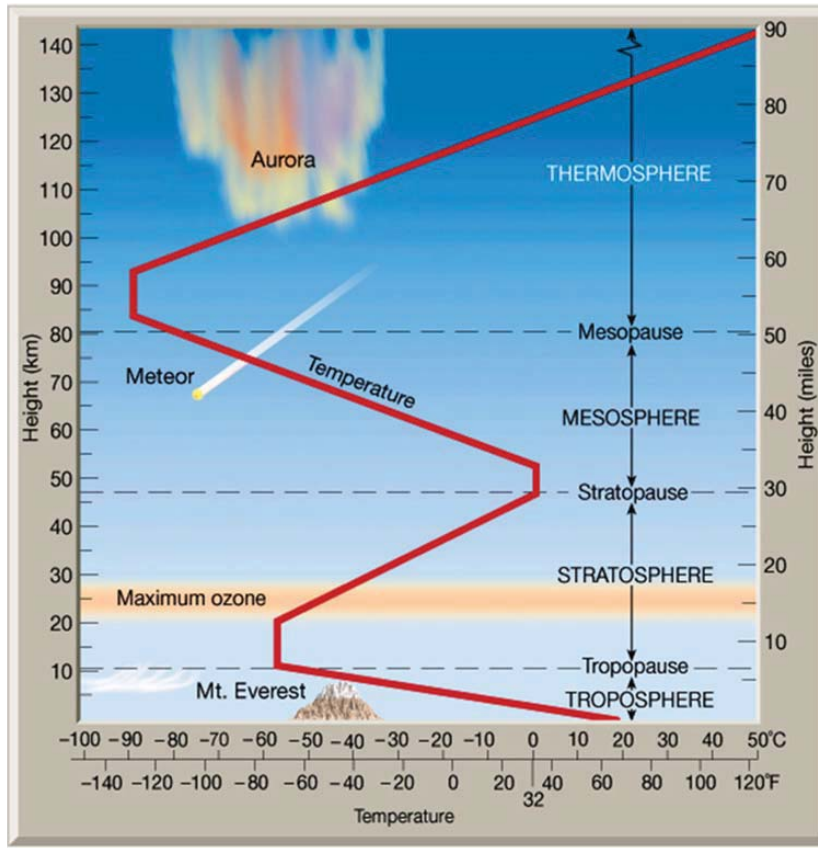

Slide 11.

The temperature lapse rate of the atmosphere is an important factor that affects greenhouse warming. There is a rapid drop of temperature from the surface to the tropopause, where the convective mixing of the atmosphere stops and the stratosphere begins. Although the pressure and temperature drop rapidly with increasing altitude in the troposphere, the entropy per unit mass of air is nearly constant, since it can only change because of the relatively slow loss of energy by radiation out of or into the air parcels. The thermal conductivity of air is much too small to permit significant heat transfer by conductivity. With no clouds, the surface can radiate directly to space in the thermal infrared window at wavelengths around 10 microns. For wavelengths outside the atmospheric window, heat is radiated to space by H_2O, CO_2 and other greenhouse molecules and by cloud tops. The more radiation to space that comes from the thermal emission of molecules or clouds at high, cold altitudes, as opposed to radiation from the warm surface or from the relatively warm lower troposphere, the more warming of the surface there will be.

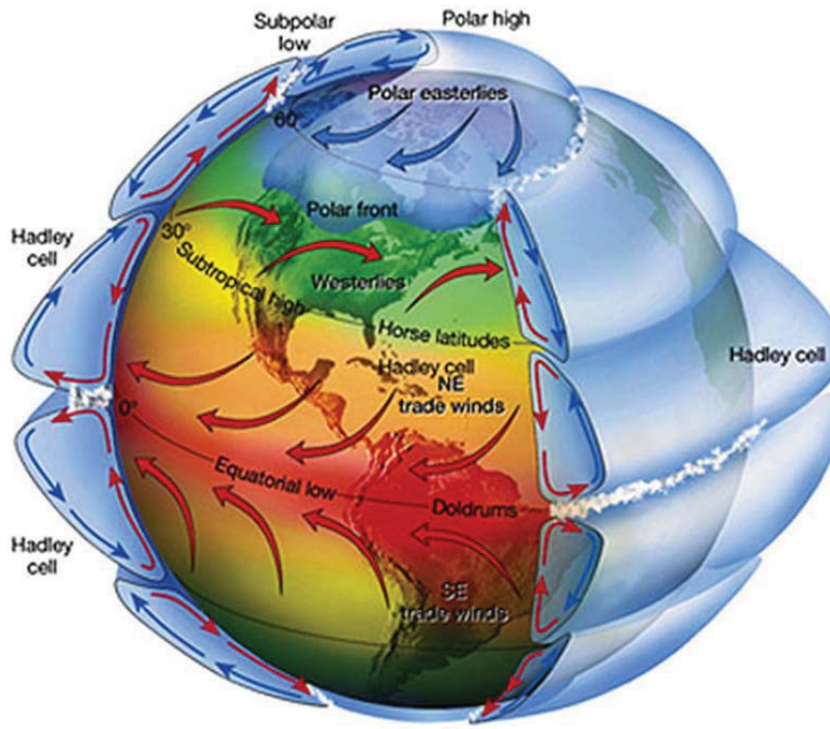

Slide 12. Atmospheric circulation.

Fluid flow in the earth's atmosphere also affects the surface temperature. Radiation into space by CO_2 and H_2O molecules cools the high-altitude branches of the enormous convective cells of air. This allows the heavier, cold (low-entropy) air to sink back to the surface of the earth. The dry air subsides at about 30 degrees latitude, north and south. These are the latitudes of the great desert belts of the earth. Because of Coriolis forces (conservation of angular momentum), the returning surface flow of air produces the easterly trade winds of the tropics, and the westerly winds of the temperate zones. Convection in the atmosphere takes heat from tropical regions to the poles and from the surface to space. The heat loss to space is entirely due to radiation from the earth's surface and from molecules and particulates at various altitudes in the atmosphere.

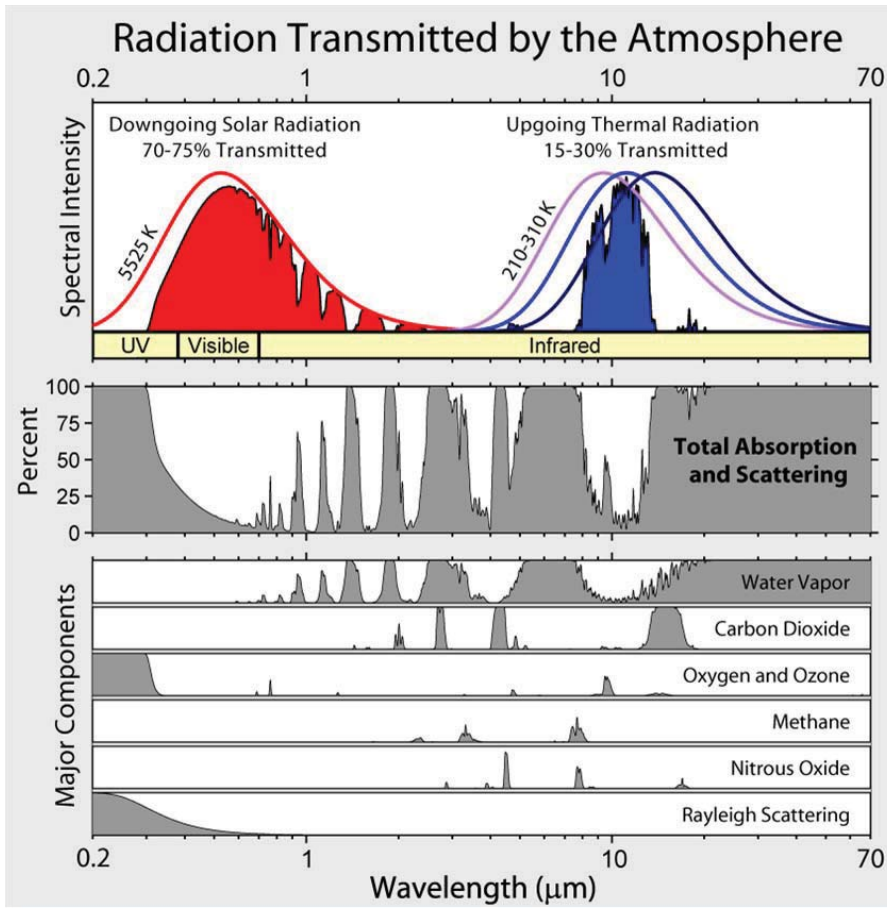

Slide 13. Radiation transmitted by the atmosphere.

There is substantial absorption of both sunlight and thermal radiation by the atmosphere, even in the absence of clouds. The shortest wavelengths of sunlight are subject to Rayleigh scattering, which makes our blue sky. Overtones of the vibrational modes of water molecules absorb substantial amounts of near infrared sunlight. Molecules of H_2O, CO_2, O_2, O_3 and others absorb so strongly in the thermal infrared that even for clear skies, only a narrow band of radiation with wavelengths near 10 microns can escape from the surface to space with no further scattering. Even though strongly absorbed frequencies cannot be radiated directly to space from the ground, they can be radiated to space by molecules at a sufficiently high altitude that the absorption by the air above them is negligible. This high-altitude radiation is weaker than it would be at the surface, since the air is cooler at higher altitudes than at the surface, and the molecules therefore do not radiate as strongly as they would if they were closer to the surface and warmer.

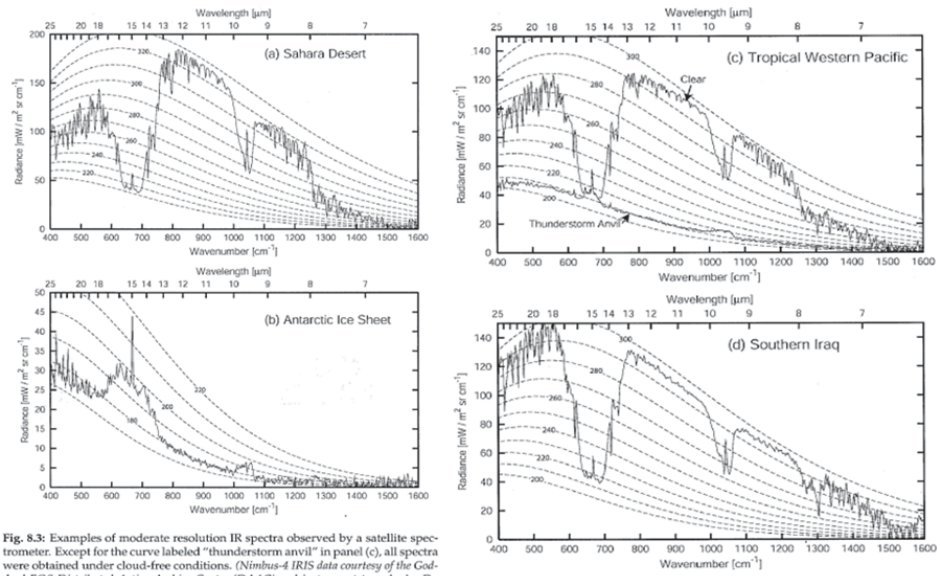

Fig. 8.3: Examples of moderate resolution IR spectra observed by a satellite spectrometer. Except for the curve labeled "thunderstorm anvil" in panel (c), all spectra were obtained under cloud-free conditions. *(Nimbus-4 IRIS data courtesy of the Goddard EOS Distributed Active Archive Center (DAAC) and instrument team leader Dr. Rudolf A. Hanel.)*

Slide 14. Examples of FTIR data from a satellite.

Unlike the model spectrum of the previous slide, these are actual experimental data, obtained from a Fourier-transform spectrometer aboard a satellite. Although generally similar to the model data, the spectra are quite different at different parts of the earth's surface. There is very little water vapor over Southern Iraq which was in dry subsiding air from the Hadley cell at the time of this measurement. There is an extreme temperature inversion over the Antarctic ice sheet, where the surface temperature is only 180 K. Over Antarctica, the CO_2 and O_2 bands show up in emission from the warmer atmosphere above the ice sheet. The atmosphere over Antarctica is so cold that it contains practically no water vapor. Finally note very weak infrared emission from the cold top of the thunderstorm anvil over the Tropical Western Pacific Ocean, the site of the celebrated "warm pool" that is involved in El Nino's and La Nina's. The suppression of infrared radiation by high, cold cloud tops, especially cirrus clouds, is a potent global warming mechanism. However, for low clouds, the increase in visible albedo is a potent cooling mechanism. We live on a partly-cloudy planet, and details of cloud cover have a huge impact on the surface temperature. The cloud cover on the day of Freeman's birthday celebration is show in the next few slides, as recorded in different wave length bands by satellites.

Visible reflected sunlight at dawn today.

0.63 micrometers.

Lots of white clouds

Darker surface areas have more solar heating.

Slide 15.
http://www.ssec.wisc.edu/data/geo/index.php

Shortwave IR.

3.9 micrometers.

More thermal emission from dark (warm) areas, surface, low cloud tops.

Less thermal emission from white (cool) areas, high cloud tops.

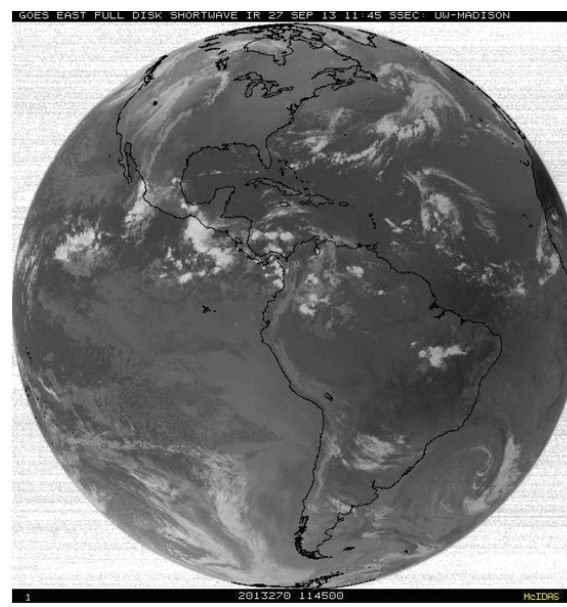

Slide 16.

Water vapor

6.5 micrometers
(bending-mode).

Very optically thick,
emission from high
altitudes,
(mid troposphere).

Dark is relatively low,
warm water vapor.

Light is higher, cold vapc
near cloud tops.
(deep convection).

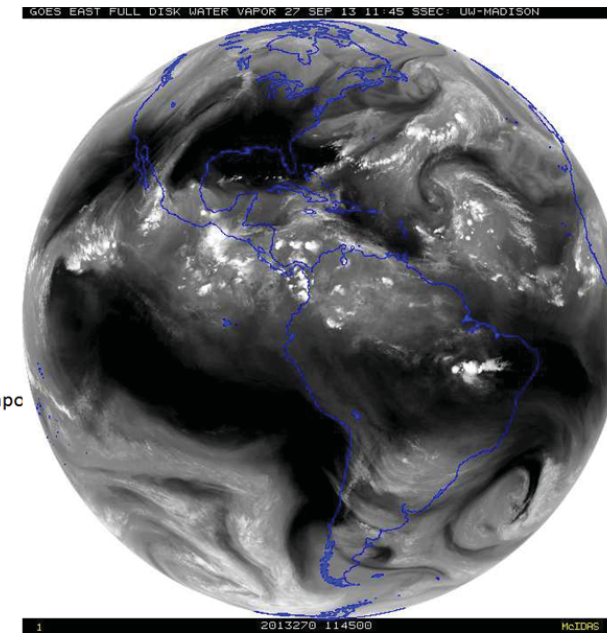

Slide 17.

Longwave IR

10.7 micrometers
(middle of IR "window")

Negligible radiation from
greenhouse gases, almost
all from surface and clouds.

White, cold cloud tops.

Darker features are low,
warm cloud tops **or** cold,
semi-transparent cirrus.

Small fraction of surface is
free of clouds.

Bottom line:
Clouds are 800 lb
Gorilla!

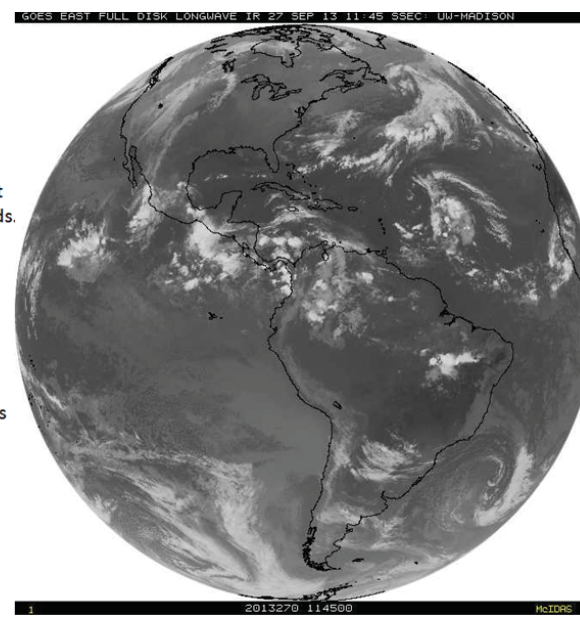

Slide 18.

A one-slide summary of climate sensitivity, the temperature increments ΔT produced by doubling CO_2 concentrations in the atmosphere is shown in Slide 19. Note the very large assumed feedback, $f = 2/3$. The feedback comes from changes in cloud cover and from the distribution of water vapor in the atmosphere. In fact the physics of these processes is so poorly known that the feedback factor could be much smaller and even negative.

Steady-State Temperature Change for Doubled CO2

$$\Delta T = \frac{T_e \Delta Q_2}{4 Q_e (1-f)} = \frac{0.305 \Delta Q_2}{1-f} \text{ K m}^2 \text{ W}^{-1} = 3.4 \text{ K}.$$

$Q_e = (1-\alpha_e) F_e/4 = \sigma \epsilon_e T_e^4 = 236$ W m^{-2} = mean radiation of earth to space.

$\alpha_e = 0.306$ albedo (mostly clouds).

$F_e = 1361$ W m^{-2} = mean solar flux at earth's orbit.

$T_e = 288$ K = mean surface temperature of Earth.

$\epsilon_e = 0.606$ = effective (contrived) emissivity of Earth for T_e.

$f = 0.25\, T_e\, \partial \ln(1-\alpha_e)/\partial T - T_e\, \partial \ln \epsilon_e / \partial T = 2/3$ (per IPCC) = feedback.

$\Delta Q_2 = 3.7$ W m^{-2} (per IPCC) = radiative forcing for doubled CO2.

IPCC values of f and ΔQ_2 give far (at least a factor of 3) too much warming. Both probably wrong!

Slide 19. Summary of global warming theory.

The CO_2 molecule has three vibrational modes: the infrared active bending mode and asymmetric stretch mode, and symmetric stretch mode, which is not infrared active. The resonance frequencies of the asymmetric stretch mode lie outside the thermal emission spectrum of the earth and also outside of most of the visible spectrum of the sun, so the asymmetric stretch mode contributes little to global warming. The frequency of the symmetric stretch mode is nearly twice the frequency of the bending mode, so there can be strong mixing of the excited bending vibration with the symmetric stretch mode. This mixing, often called Fermi resonance, since it was first explained by Enrico Fermi, makes CO_2 a more potent greenhouse gas.

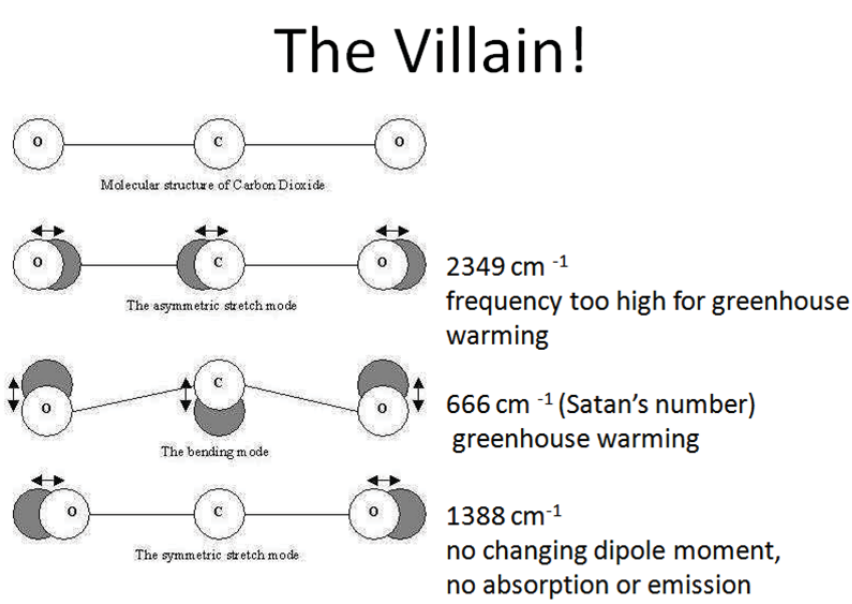

Slide 20.

Each of the strongly negative O atoms of the CO_2 molecule has a net negative charge, leaving the C atom in the middle positively charged with about half the elementary charge (the charge of a proton). It is the accelerations of these charges during the vibration and rotation of the CO_2 molecule that allows it to absorb and emit radiation. Those vibrations and rotations that produce changing electric dipole moments radiate most efficiently, very much like the whip antenna an a automobile, which also transmits and receives electric dipole radiation.

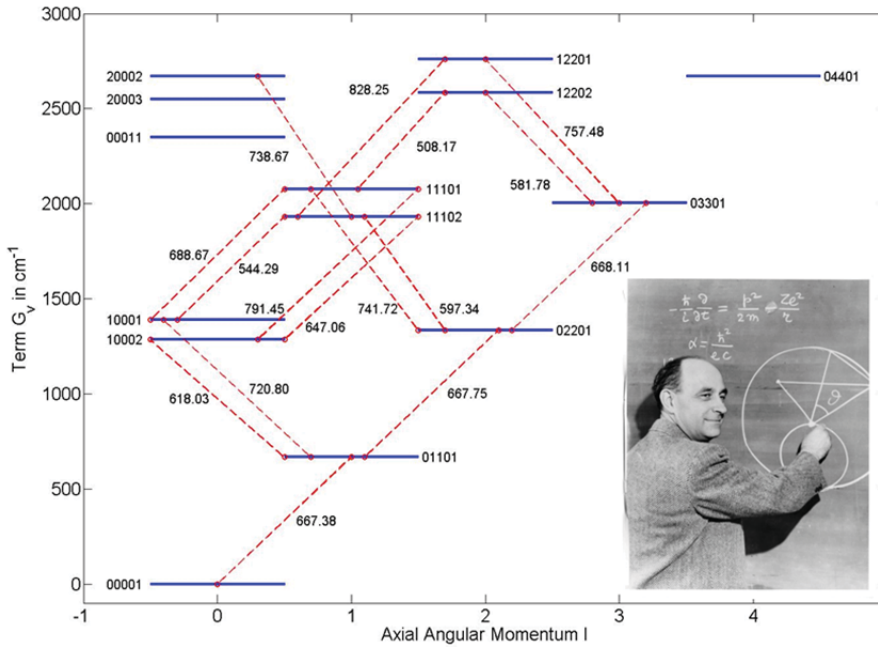

Slide 21. Fermi resonances.

The low-lying vibrational levels of the CO_2 molecule for the most abundant isotopomer $^{16}O^{12}C^{16}O$, or 626. Note the splitting of the higher bending modes by Fermi resonance interactions with the symmetric stretch mode, and with the asymmetric stretch mode. The transition frequencies for a non-rotating molecule are indicated in cm^{-1}. The states are labeled with the HITRAN code, for which the integers, reading from left to right, mean: (1) v_1 = quanta of symmetric stretch vibration; (2) v_2 = quanta of bending-mode vibration; (3) l = quanta of "vibrational" angular momentum around the axis of symmetry; (4) v_3 = quanta of asymmetric stretch vibration; (5) r = ranking index for multiplets split by Fermi mixing.

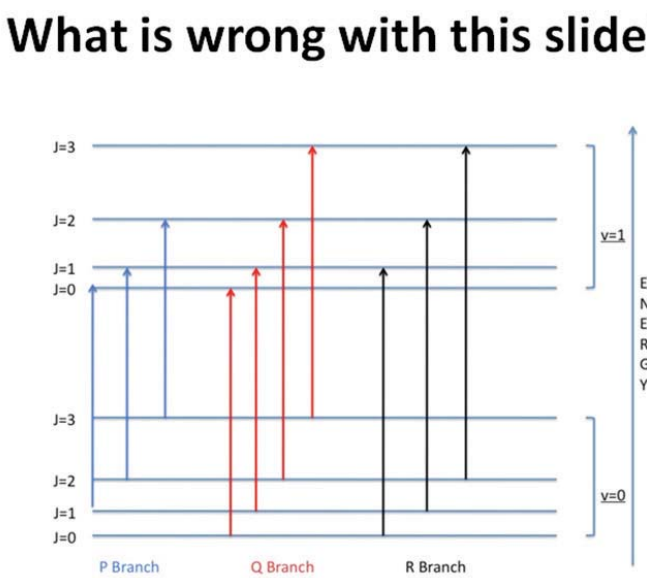

Slide 22. Schematic diagram of P, Q, and R branch transitions.

Each possible vibrational transition frequency is split into many hundreds of lines (sidebands) by the rotation of the molecule. The total angular momentum J of the molecule is a good quantum number. If J′ is the rotational quantum number of the upper vibrational state and J is the rotational quantum number of the lower vibrational state, transitions for which $J' = J - 1$ are called P transitions, transitions with $J' = J$ are called Q transitions, and transitions with $J' = J + 1$ are called R transitions. For the bending mode of the CO_2 molecule, the frequencies of the Q transitions, which corresponds to rotation of the molecule around the axis of transverse vibration, have little dependence on the rotational quantum number J of the lower state, are nearly the same as for a non-rotating molecule. The P and R transitions have lower and higher frequencies, respectively, than the non-rotating molecule, and the frequencies depend strongly on the rotational quantum number J of the lower state.

This sketch shows transitions between two vibrational states with axial angular momentum $L = 0$, for example, for the asymmetric stretch state of the CO_2 molecules where the electric dipole moment is along the symmetry axis. For the bending mode of CO_2, that contributes to global warming, the electric dipole moment is perpendicular to the symmetry axis, and the axial angular momentum quantum numbers, L′ and L, of the upper and lower states must differ by one unit, that is $L' = L + 1$ or $L' = L - 1$, as illustrated on the previous slide. If the O atoms are identical, the states $L = 0$ and odd J are missing because of exchange symmetry. States with nonzero L and non-identical O atoms are narrow parity doublets.

Attenuation Coefficient (e-foldings / length)

$$\kappa = N \sum_{eg} \sigma_{eg} = N \sum_{eg} S_{eg} G_{eg}$$

N is the number density of CO_2 molecules, and σ_{eg} is the cross section of the transition from a lower state g to an upper state e; G_{eg} is the lineshape function.

Line strength (in cm)

$$S_{eg} = \frac{8\pi^3 \nu_{eg} |D_{eg}|^2 e^{-E_g/kT} \left(1 - e^{-hc\nu_{eg}/kT}\right)}{hcZ}$$

ν_{eg} = frequency (in cm^{-1}) of the transition, D_{eg} = the electric dipole matrix element, E_g = lower-state energy, T = absolute temperature, k = Boltzmann's constant, h = Planck's constant, c = speed of light, T = absolute temperature.

Partition function

$$Z = \sum_j e^{-E_j/kT}$$

Slide 23.

The important line strength factor S_{eg} is a bit like a temperature-dependent "oscillator strength." It takes into account both absorption and stimulated emission of molecules that are in thermal equilibrium at a temperature T. Since it is not possible to calculate the matrix element D_{eg} of the electric dipole moment with sufficient accuracy for them to be of use in modeling the greenhouse effect, line strength factors are measured and tabulated, often at a reference temperature of 296 K, as in the HITRAN data base.

To get absorption cross sections it is necessary to have line shape factors G_{eg} as well as line strength factors. The line strength factors S_{eg} have been determined very well by experiment. The line shape factors G_{eg} have been determined experimentally to be very nearly Lorentzian (or Doppler-broadened Lorentizian = Voigt profiles) near line centers, but very little is known experimentally about the far wings of the profiles.

Normalized line shapes

$$\int_0^\infty G_{eg} d\nu = 1$$

A Lorentzian line shape

$$G_{eg} = \frac{\mu_{eg}/\pi}{\mu_{eg}^2 + (\nu - \nu_{eg})^2}$$

μ_{eg} = broadening; ν = frequency; ν_{eg} = resonance.

A Voigt line shape

$$G_{eg} = \frac{\mu_{eg}}{\pi}\sqrt{\frac{m}{2\pi kT}}\int_{-\infty}^{\infty}\frac{e^{-mv^2/2kT}dv}{\mu_{eg}^2 + (\nu - \nu_{eg}[1 + v/c])^2}$$

Slide 24.

The intrinsic line shapes of vibration-rotation transitions of the CO_2 molecule in the earth's atmosphere are almost completely determined by collisions, except for the high stratosphere where Doppler broadening of the lines is no longer negligible, and one should use a Voigt profile near line center.

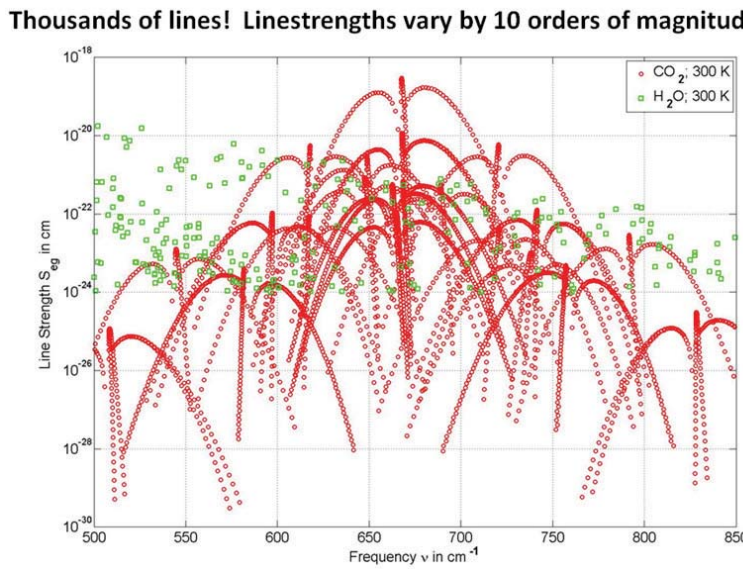

Slide 25.

Line strengths have been carefully measured for many transitions of CO_2, H_2O and other atmospheric molecules. This shows some of the strengths of the strongest lines of CO_2 and of H_2O lines in the same spectral region. To get accurate radiative forcing from line strengths requires that we know the lineshape functions very well. This is especially true of CO_2 where the lines in the center of the band are some six orders of magnitude stronger than the lines at the edge of the band, which contribute to changes in radiative forcing with changing CO_2. The sharp cascades of strengths correspond to Q branches, and the "angel wings" to the left and right of the Q branch are the corresponding P and R branches. Especially for low frequencies, there is strong of overlap of lines from CO_2 and H_2O.

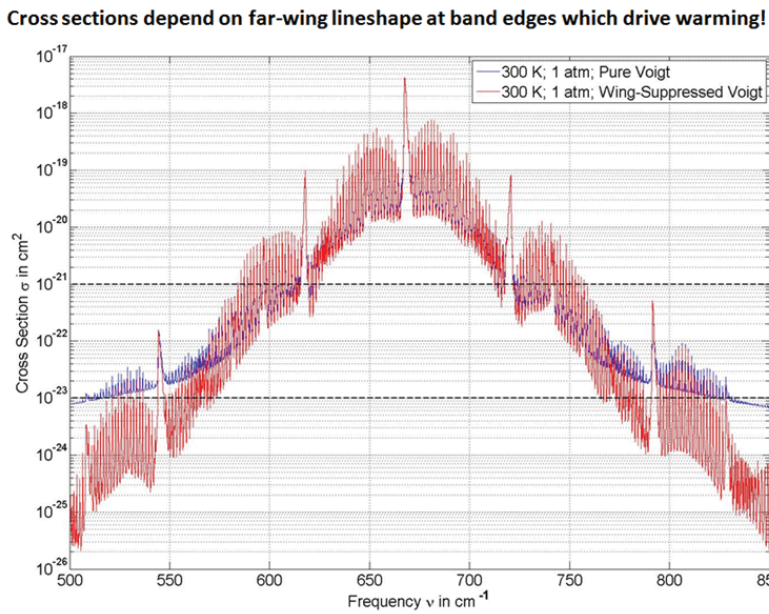

Slide 26.

Assuming Voigt line shapes greatly overestimates the net CO_2 cross section in the wings of the band. Cross sections with value between 10^{-23} and 10^{-21} cm^2 are responsible for almost all of the greenhouse warming from additional CO_2. Current column density of CO_2 is 8.6×10^{21} cm^{-2}.

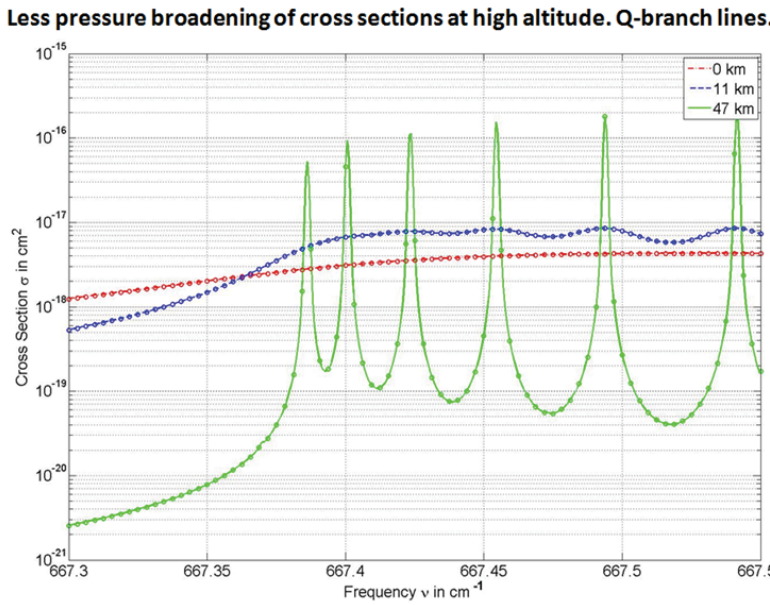

Slide 27.

This is a fine-scale plot of the absorption cross section for CO_2 near the very center of the 667 band. The resonances are for Q-branch ($J' - J = 0$) transitions from rotational states with angular momentum quantum numbers $J = 0, 2, 4, \ldots$ of the ground vibrational level to the first excited vibrational level of the the most abundant isotopomer $^{16}O^{12}C^{16}O$ or 626. Because the O nuclei are identical bosons, the rotational levels with odd J are missing. Pressure broadening at the earth's surface smears out the resonance lines, but they are well resolved at the top of the stratosphere, 47 km, where the pressure is only a few millibar. The continuous lines are for Voigt profiles, and the points are Voigt profiles with suppressed wings. Wing suppression makes no difference at the center of the absorption band.

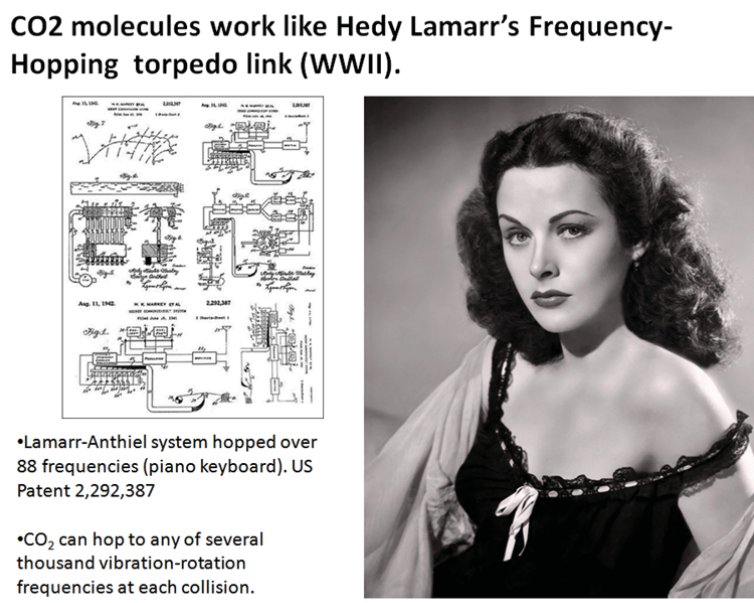

Slide 28.

One can think of individual CO_2 molecules as spread-spectrum emitters and absorbers of infrared radiation. The far-wing lineshapes, and the global-warming potential of CO_2 molecules, depend on how fast the frequency of the CO_2 molecule hops from one value to another. One of the first spread-spectrum patents was co-written by the actress Hedy Lamarr and the composer and pianist George Anthiel before World War II.

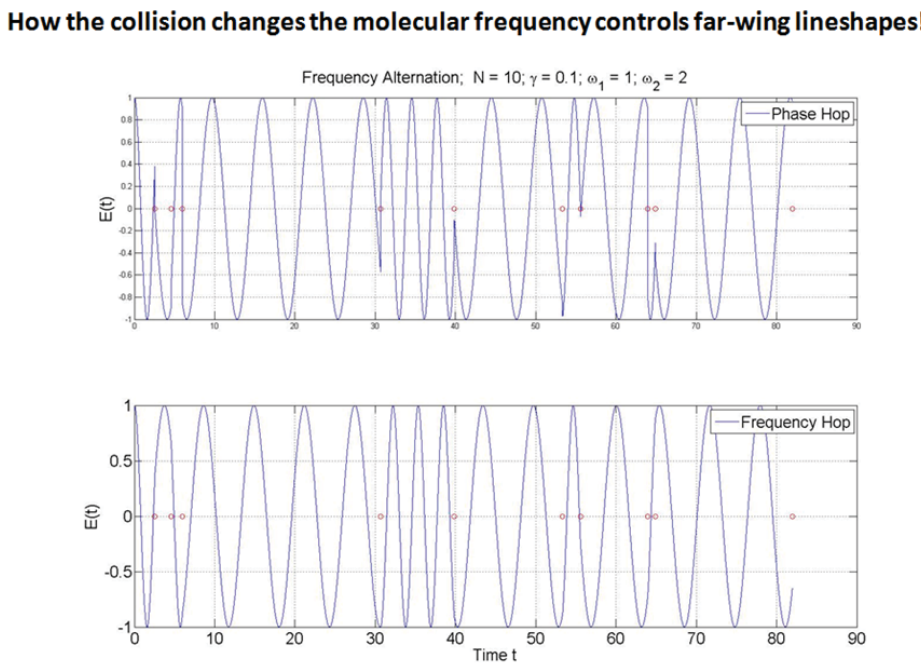

Slide 29.

The classical Lorentzian line shape is produced when the frequency-changing collisions produce a discontinuity in the phase or amplitude of the oscillation. The far-wing line shape is substantially different if the frequency-changing collisions keep the phase continuous or if they take a finite time to shift the amplitude. For slow frequency hopping, the far wings of the line shape function fall off as the inverse fourth power of the detuning, much more rapidly than the far wings of Lorentzian lines, which fall off as the inverse square of the detuning.

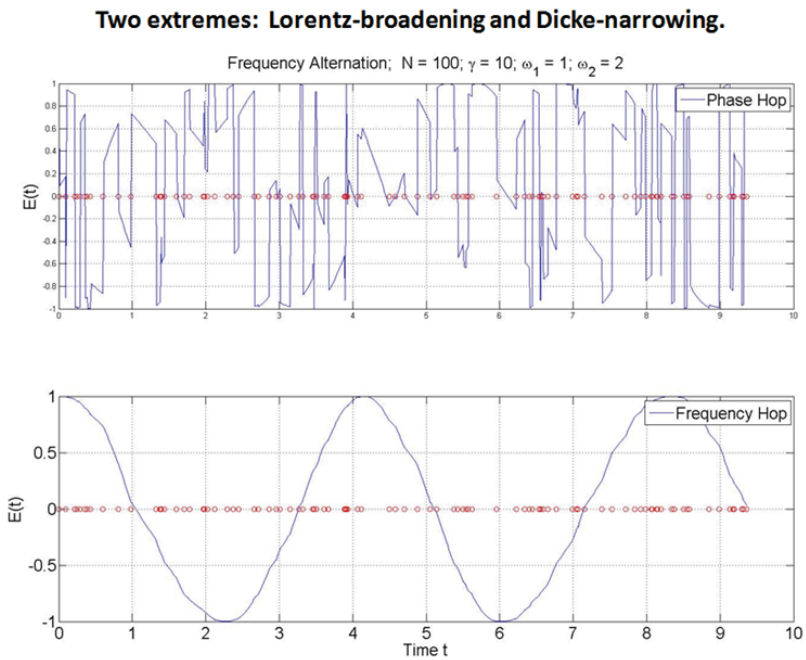

Slide 30.

The difference between instantaneous phase hops and instantaneous frequency hops is especially dramatic in the idealized limit of many collisions per oscillation period. Rapid phase hopping collisions produce a very broad line with no remaining frequency structure. Rapid frequency hopping leads to motional (Dicke) narrowing. Then the molecule emits or absorbs radiation as a sharp line centered at the average frequency of the collisionally-coupled transitions.

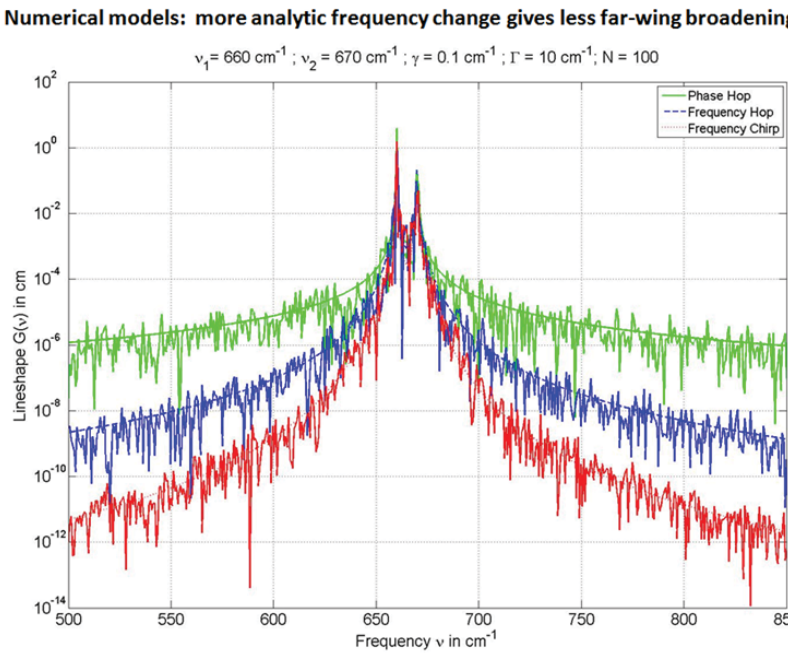

Slide 31.

The Lorentzian line is produced by instantaneous phase hops, which make no physical sense. For Lorentzian lines, the far wings fall off as the inverse square of the detuning. In fact, collisions of CO_2 molecules with N_2 or O_2 molecules of the air are not instantaneous but take a few picoseconds (10^{-12} s). For instantaneous frequency hops, the lineshapes fall off as the inverse fourth power of the detuning. If one models lineshapes for a linear chirp from an initial to a final frequency, the far wing lines are found to fall off as the inverse sixth power of the detuning. The "speckle noise" is characteristic of numerical modelling of spectra with random phase hops, frequency hops, frequency chirps, etc. The speckle intensities have a decaying exponential distribution (a Raleigh distribution) just like that of laser or radar speckle.

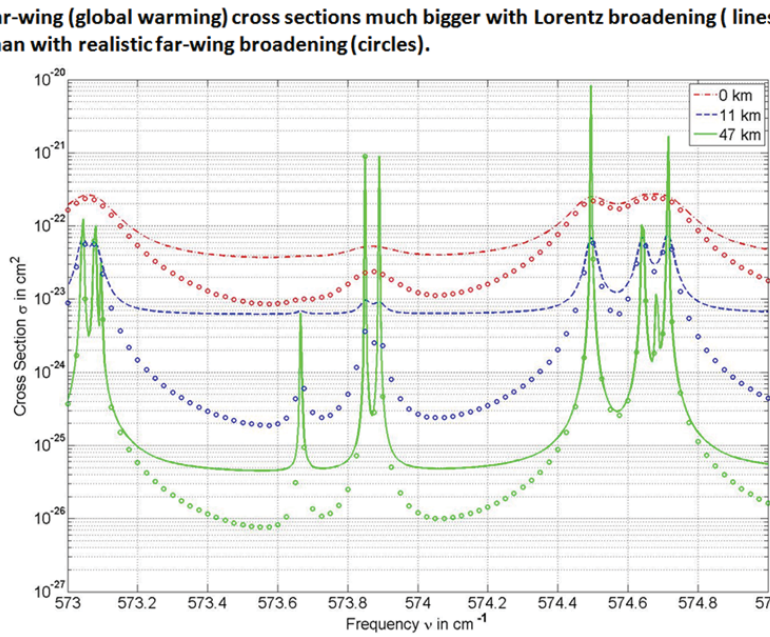

Slide 32.

Cross sections in the wings of the 667 absorption band of CO_2. Much of the absorption between resonance lines comes from the wings of the strong lines near the center of the band. The continuous curves are for Voigt profiles and the points are for wing-suppressed Voigt profiles. Most of the resonance lines are for P ($J' - J = -1$) and R ($J' - J = 1$) transitions out of high vibrational states of the most abundant isotopomer $^{16}O^{12}C^{16}O$ or 626, but the weak resonance at 573.666 comes from the next-most abundant isotopomer $^{16}O^{13}C^{16}O$ or 636.

Radiation transfer details:

Schwartzschild equation for radiant intensity from earth.

$$I(\infty) = I(0)e^{-\tau(0)} + \int_0^\infty e^{-\tau} B\kappa dz.$$

Planck brightness

$$B = \left(\frac{2\epsilon^3}{c^2h^2}\right)\frac{1}{e^{\epsilon/kT} - 1}$$

Attenuation rate

$$\kappa = \sigma_{eg}N_g - \sigma_{ge}N_e.$$

Optical depth to space

$$\tau = \int_z^\infty \kappa(z')dz',$$

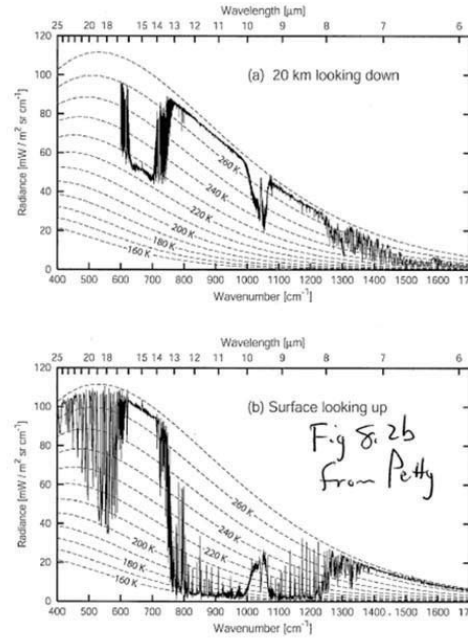

Fig. 8.2: Coincident measurements of the infrared emission spectrum of the cloud-free atmosphere at (a) 20 km looking downward over the polar ice sheet and (b) at the surface looking upward. *(Data courtesy of David Tobin, Space Science and Engineering Center, University of Wisconsin-Madison.)*

Slide 33.

The measured spectra of thermal radiation looking down at the earth through cloud-free air is a "mirror image" of the spectrum observed from the surface looking up. Looking down, one sees the relatively warm surface in the infrared window, cold CO_2 in the lower stratosphere and a narrow spike of CO_2 emission in the upper stratosphere from extremely intense Q branch at the center of the band. Looking up, one sees the cold outer space in the infrared window, relatively warm CO2 directly overhead. The narrow Q branch looking up is probably from even warmer CO_2 in the laboratory. At the 667.5 cm^{-1} peak of the Q branch the e-folding length is 11 cm, about 4 inches at the surface.

Downwelling Flux at the Surface

$$J(0) = \int_0^\infty \kappa(z) B(z) e^{-\rho(z)} dz$$

Planck Brightness

$$B = \frac{2hc^2\nu^3}{e^x - 1}, \quad \text{where} \quad x = \frac{hc\nu}{kT}$$

Optical Depth from Surface to Altitude z

$$\rho(z) = \int_0^z \kappa(z')dz'$$

Slide 34.

The basic radiative transfer equations describe the net effect of spontaneous and stimulated emission and of absorption by molecules. Quite similar equations describe the gain of lasers, where the distribution of the molecules over the quantized energy states is far from thermal equilibrium and one can get gain.

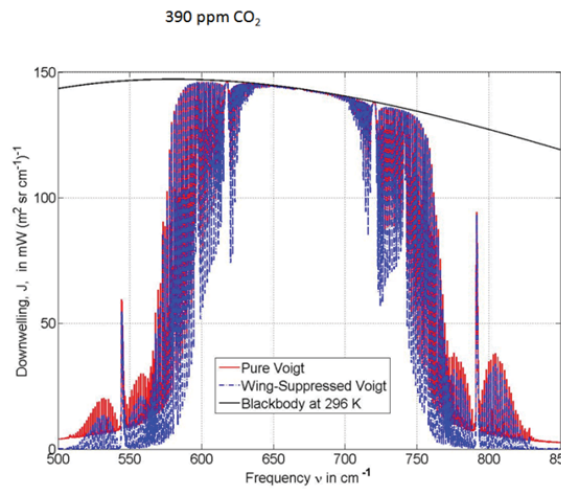

Slide 35.

This is a modelled downwelling spectrum at the earth's surface. It comes from CO_2 in a cloud-free atmosphere with no other greenhouse molecules, notably no H_2O. The assumed line profile makes very little difference near the center of the band, but it makes a big difference in the far wings. The assumed CO_2 concentration, 390 ppm, is close to today's value.

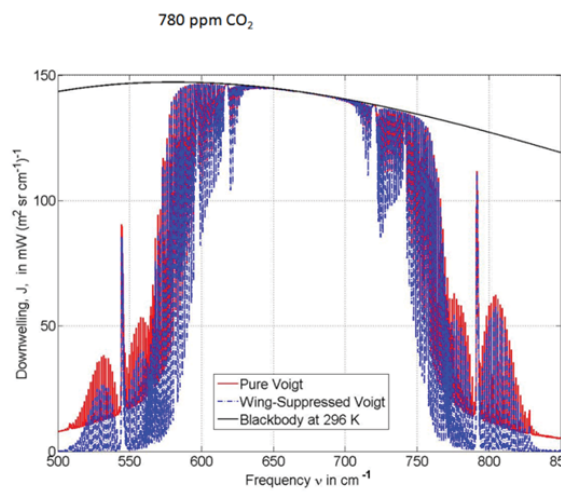

Slide 36.

This is modelled in the same way as for the previous slide, only with twice the CO_2 concentration. Doubling the CO_2 concentration makes no difference near line center, but it does add more downwelling radiation in the wings.

Using Voigt profiles increases the radiative-forcing increment from doubling CO_2 by a factor of ∼1.4, but far wing absorption from Voigt profiles does not exist!

Voigt Line Shapes Don't Work in Far Wings!

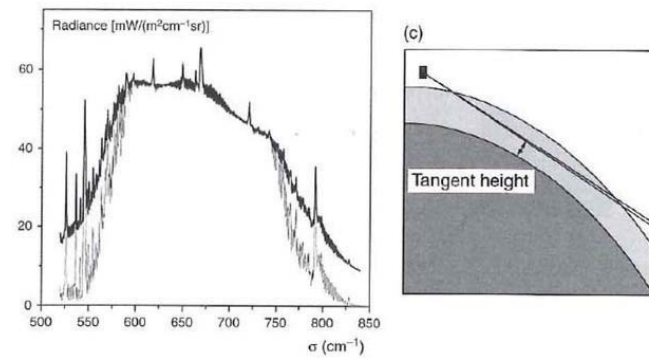

Fig. VII.15: Radiance emitted by the Earth atmosphere in the region of the ν_2 CO_2 band for a 1 cm^{-1} resolution. The thin line gives measured values obtained by a balloon-borne instrument[29] at 40 km altitude looking down to a tangent height of 10 km. The thick line corresponds to predictions using purely Voigt line shapes. After Ref. 603.

Hartmann, Boulet and Robert, *Collisional Effects on Molecular Spectra, Elsevier, 2008*

Slide 37.

The inadequacies of the Voigt profile for far-wings of the CO_2 band have already been demonstrated experimentally many times. A recent example is the balloon observations cited in the recent book by Hartmann *et al.*

Happy 90th Birthday Freeman!

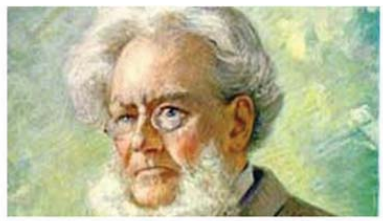

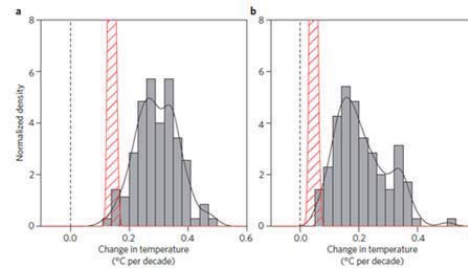

Figure 1 | Trends in global mean surface temperature. **a**, 1993-2012. **b**, 1998-2012. Histograms of

- "I am in revolt against the age-old lie that the majority is always right."

Henrik Ibsen, *An Enemy of the People*

Slide 38.